

# Superheavy Element Flerovium (Element 114) is a Volatile Metal

Alexander Yakushev<sup>†,‡,⊘</sup>, Jacklyn M. Gates<sup>†,‡,♦</sup>, Andreas Türler<sup>†,‡,♦</sup>, Matthias Schädel<sup>‡,♥</sup>, Christoph E. Düllmann<sup>‡,§,⊘,\*</sup>, Dieter Ackermann<sup>‡</sup>, Lise-Lotte Andersson<sup>‡</sup>, Michael Block<sup>‡</sup>, Willy Brüchele<sup>‡</sup>, Jan Dvořák<sup>‡,♦</sup>, Klaus Eberhardt<sup>§</sup>, Hans G. Essel<sup>‡</sup>, Julia Even<sup>§</sup>, Ulrika Forsberg<sup>∇</sup>, Alexander Gorshkov<sup>†,⊘</sup>, Reimar Graeger<sup>†,⊘</sup>, Kenneth E. Gregorich<sup>‡</sup>, Willi Hartmann<sup>‡</sup>, Rolf-Dietmar Herzberg<sup>‡</sup>, Fritz P. Heßberger<sup>‡,⊘</sup>, Daniel Hild<sup>§</sup>, Annett Hübner<sup>‡</sup>, Egon Jäger<sup>‡</sup>, Jadambaa Khuyagbaatar<sup>‡,⊘</sup>, Birgit Kindler<sup>‡</sup>, Jens V. Kratz<sup>§</sup>, Jörg Krier<sup>‡</sup>, Nikolaus Kurz<sup>‡</sup>, Bettina Lommel<sup>‡</sup>, Lorenz J. Niewisch<sup>§</sup>, Heino Nitsche<sup>‡,♦</sup>, Jon Petter Omtvedt<sup>×</sup>, Edward Parr<sup>‡</sup>, Zhi Qin<sup>∇</sup>, Dirk Rudolph<sup>∇</sup>, Jörg Runke<sup>‡</sup>, Brigitta Schausten<sup>‡</sup>, Erwin Schimpf<sup>‡</sup>, Andrey Semchenkov<sup>×</sup>, Jutta Steiner<sup>‡</sup>, Petra Thörle-Pospiech<sup>§,⊘</sup>, Juha Uusitalo<sup>#</sup>, Maciej Wegrzecki<sup>‡</sup>, Norbert Wiehl<sup>§,⊘</sup>

<sup>†</sup>Institut für Radiochemie, TU Munich, 85748 Garching, Germany; <sup>‡</sup>Abteilung SHE Chemie, GSI Helmholtzzentrum für Schwerionenforschung, 64291 Darmstadt, Germany; <sup>§</sup>Institut für Kernchemie, Johannes Gutenberg University Mainz, 55099 Mainz, Germany; <sup>⊘</sup>Sektion SHE Chemie, Helmholtz Institute Mainz, 55099 Mainz, Germany; <sup>‡</sup>Department of Physics, University of Liverpool, L69 7ZE Liverpool, UK; <sup>‡</sup>Nuclear Science Division, Lawrence Berkeley National Laboratory, Berkeley, CA 94720-8169, U.S.A.; <sup>♦</sup>Chemistry Faculty, University of California, Berkeley, CA 94720-1460, U.S.A.; <sup>∇</sup>Department of Physics, Lund University, 221 00 Lund, Sweden; <sup>×</sup>Department of Chemistry, University of Oslo, 0315 Oslo, Norway; <sup>∇</sup>Institute of Modern Physics, 730000 Lanzhou, P.R. China; <sup>#</sup>Department of Physics, University of Jyväskylä, 40014 Jyväskylä, Finland; <sup>♥</sup>Institute of Electron Technology, 02-668 Warsaw, Poland

---

Element 114 / Flerovium / Gas phase chromatography / Single atom chemistry / Relativistic effects

---

Supporting Information Placeholder

**ABSTRACT:** The electron shell structure of superheavy elements, i.e., elements with atomic number  $Z \geq 104$ , is influenced by strong relativistic effects caused by the high  $Z$ . Early atomic calculations on element 112 (copernicium, Cn) and element 114 (flerovium, Fl) having closed and quasi-closed electron shell configurations of  $6d^{10}7s^2$  and  $6d^{10}7s^27p_{1/2}$ , respectively, predicted them to be noble gas-like due to very strong relativistic effects on the  $7s$  and  $7p_{1/2}$  valence orbitals. Recent fully relativistic calculations studying Cn and Fl in different environments suggest them to be less reactive compared to their lighter homologs in the groups, but still exhibiting a metallic character. Experimental gas-solid chromatography studies on Cn have, indeed, revealed a metal-metal bond formation with gold. In contrast to this, for Fl, the formation of a weak bond upon physisorption on gold was inferred from first experiments. Here, we report on a gas-solid chromatography study of the adsorption of Fl on a gold surface. Fl was produced in the nuclear fusion reaction  $^{244}\text{Pu}(^{48}\text{Ca}, 3\text{-}4n)^{288,289}\text{Fl}$  and was isolated in-flight from the primary  $^{48}\text{Ca}$  beam in a physical recoil separator. The adsorption behavior of Fl, its nuclear  $\alpha$ -decay product Cn, their lighter homologs in groups 14 and 12, i.e., Pb and Hg, and the noble gas Rn were studied simultaneously by isothermal gas chromatography and thermochromatography. Two Fl atoms were detected. They adsorbed on a gold surface at

room temperature in the first, isothermal part, but not as readily as Pb and Hg. The observed adsorption behavior of Fl points to a higher inertness compared to its nearest homolog in the group, Pb. However, the measured lower limit for the adsorption enthalpy of Fl on gold points to the formation of a metal-metal bond of Fl with gold. Fl is the least reactive element in the group, but still a metal.

## 1. Introduction

Superheavy elements (SHE) are unique in two respects. Their nuclei exist only due to nuclear shell effects, and their electron structure is influenced by increasingly important relativistic effects.<sup>1-3</sup> Syntheses of SHE with proton number  $Z$  up to 118 have been reported.<sup>4</sup> Elements with  $Z=104$ -112 are members of the  $6d$  series in the Periodic Table of the Elements. The  $7p$  valence shell is expected to be filled in the elements with  $Z=113$ -118. The discovery of elements with  $Z=114$  and  $Z=116$  was recently officially accepted and they were named flerovium (Fl) and livermorium (Lv), respectively.<sup>5</sup> Lighter transactinides with  $Z = 104$ -108 were experimentally shown to be members of groups 4 through 8 of the

Periodic Table of the Elements.<sup>6</sup> Due to the increasing nuclear charge in SHE the velocity of electrons in the inner shells approaches the speed of light. This causes a relativistic increase in the electron mass. Hence, the spherical  $s$  and  $p_{1/2}$  electron shells, having a non-zero electron density at the nucleus, contract in space and become stabilized in energy. This is the so-called direct relativistic effect. As a consequence, the non-spherical atomic orbitals (AOs)  $p_{3/2}$ ,  $d$ ,  $f$ , etc. are more efficiently screened from the nucleus, thus undergoing destabilization in energy and expansion in space: the indirect relativistic effect. Finally, the third effect is a spin-orbit splitting of AOs with  $l > 0$ . All three relativistic effects scale approximately with  $Z^2$  for valence electron shells and are thus most pronounced in SHE.

Beyond the classical closed-shell configuration  $6d^{10}7s^2$  in copernicium (Cn, element 112), the very large spin-orbit splitting in  $7p$  AOs and the strong relativistic stabilization of the  $7p_{1/2}$  AOs results in a quasi-closed-shell configuration  $7s^27p_{1/2}^2$  in flerovium. This, together with the relativistic stabilization of the  $7s$  AOs renders both Cn and Fl to be more inert than their lighter homologs. According to early atomic calculations by Pitzer<sup>7</sup>, the promotion energy to the valence state electron configuration  $s^2 \rightarrow sp$  in Cn and  $p_{1/2}^2 \rightarrow p^2$  in Fl will not be compensated by the energy gain of the chemical bond formation. He concluded that both Cn and Fl are very inert, like noble gases or volatile liquids bound by dispersion forces only. At the same time other approaches, e.g., extrapolations along group 12 and 14 indicate a noble, but metallic character for these elements, more similar to their homologs mercury and lead, respectively.<sup>8</sup>

The discovery of neutron-rich isotopes of Cn and Fl with half-lives,  $T_{1/2}$ , in the range of seconds<sup>9</sup> aroused new interest for theoretical predictions of the adsorption behavior for Cn and Fl on various surfaces and called for first experimental efforts. Eichler quantified the adsorption interaction of the hypothetically noble metals Cn and Fl with transition metal surfaces<sup>10</sup> based on an empirical model developed by Midema and Nieuwenhuys.<sup>11</sup> Adsorption enthalpies of Fl on different transition metal surfaces were predicted to be higher by approximately  $100 \text{ kJ}\cdot\text{mol}^{-1}$  than those of Cn on these surfaces.<sup>10</sup> Experimental studies on the adsorption of Rn on various transition metal surfaces were undertaken, serving as a model for a hypothetical *noble-gas-like* behavior of elements Cn and Fl<sup>12</sup>. The authors of ref. 12 applied an extended Midema-model for estimating the strength of Cn and Fl adsorption on those metals. The adsorption of Fl on a metal surface was predicted to be stronger than that of Cn. However, if Cn and Fl would exhibit *noble-gas-like* properties, their adsorption enthalpy values would be much lower than in the case of a *noble-metal-like* behavior.<sup>12</sup> More recent molecular, cluster, and solid-state relativistic calculations on these elements suggest Cn and Fl to be more inert than their lighter homologs in the groups, but still reveal a metallic character<sup>13-15</sup>, e.g., in  $MM'$  interactions ( $M = \text{Cn or Fl}$ ,  $M' = \text{metal}$ , e.g., Au). In contrast to Pitzer's conclusion, Fl is now expected to provide both  $7p_{1/2}$  and  $7p_{3/2}$  AOs for metal-metal interactions. By considering the hypothetical solid state of Fl, the authors of ref. 16 found that Fl is the most inert element in group 14, but reveals a metallic character, with the cohesive energy being  $0.5 \text{ eV/atom}$ . Therefore, a purely van der Waals type interaction upon adsorption on metal surfaces, as is typical for noble gases is no longer anticipated for either element. Hence, the determination of the adsorption enthalpy of the interaction of Cn and Fl with metal surfaces

is a suitable experimental method to discriminate between a *noble-gas-like* and a *noble-metal-like* behavior. The adequate experimental approach is detection of atoms (molecules) adsorbed inside a gas-chromatography channel within a broad temperature range. The chromatography channel is made of silicon detectors for the detection of  $\alpha$  particles and spontaneous fission (SF) fragments. This approach was successfully applied for the first time in chemical studies on  $\text{HsO}_4$ .<sup>17</sup> Cn was investigated by thermochromatography on a gold surface. Five  $\alpha$ -SF decay chains starting with  $^{283}\text{Cn}$  were found by irradiating a  $^{242}\text{Pu}$  target with a  $^{48}\text{Ca}$  ion beam.<sup>18,19</sup> The evaluated adsorption enthalpy of Cn on Au ( $-\Delta H_{\text{ads}}^{\text{Au}}(\text{Cn}) = 52_{-3}^{+4} \text{ kJ}\cdot\text{mol}^{-1}$ , at the 68% confidence level (68% c.l.), points at the formation of a weak metal-metal bond with Au<sup>19</sup>. The determined adsorption enthalpy value for Cn is significantly lower than that for the nearest homolog in the group Hg ( $-\Delta H_{\text{ads}}^{\text{Au}}(\text{Hg}) = 98 \pm 3 \text{ kJ}\cdot\text{mol}^{-1}$ , ref. 20); however in agreement with the limit ( $-\Delta H_{\text{ads}}^{\text{Au}}(\text{Cn}) < 60 \text{ kJ}\cdot\text{mol}^{-1}$ ) which was found in previous experiments.<sup>21</sup> Thus, Cn exhibits *noble-metal-like* properties<sup>18,19</sup>, in line with trends established by the lighter homologues in group 12, and in good agreement with recent theoretical calculations.<sup>14,15</sup>

In recent years, Fl isotopes with half-lives of the order of seconds have been discovered.<sup>9,22-26</sup> The most long-lived currently known Fl isotopes, produced in the nuclear fusion reaction  $^{48}\text{Ca} + ^{244}\text{Pu}$ , are  $^{289}\text{Fl}$  ( $T_{1/2} = 2.1 \text{ s}$ ) and  $^{288}\text{Fl}$  ( $T_{1/2} = 0.69 \text{ s}$ ), which are formed upon the evaporation of three or four neutrons from the excited compound nucleus, respectively. These half-lives are long enough for current gas phase chromatography experiments with single atoms of superheavy elements.<sup>6</sup> Besides the short half-lives, minute production rates<sup>4,22</sup> also complicate chemical studies of superheavy elements. Beyond Cn, only a single chemical experimental study, focused on Fl, is reported to date.<sup>27</sup> Three atoms from two Fl isotopes,  $^{287,288}\text{Fl}$ , were found to pass gold surfaces kept at room temperature and progressively getting colder, until they adsorbed at temperatures of  $-88^\circ \text{C}$ ,  $-90^\circ \text{C}$  and  $-4^\circ \text{C}$ . A Monte-Carlo simulation of the observed adsorption behavior resulted in  $-\Delta H_{\text{ads}}^{\text{Au}}(\text{Fl}) = 34_{-11}^{+54} \text{ kJ}\cdot\text{mol}^{-1}$  at the 95% confidence level (95% c.l.). The rather low most probable value of  $-\Delta H_{\text{ads}}$  was interpreted by the authors as evidence for the formation of a weak physisorption bond between atomic Fl and a gold surface.<sup>27</sup> However, the large uncertainty of the reported  $-\Delta H_{\text{ads}}$  covers almost the entire range from a typical *metallic* (cf.  $-\Delta H_{\text{ads}}^{\text{Au}}(\text{Hg}) = 98 \pm 3 \text{ kJ}\cdot\text{mol}^{-1}$ , ref. 20) to a *noble-gas-like* behavior (cf.  $-\Delta H_{\text{ads}}^{\text{ice}}(\text{Rn}) = 19.2 \pm 1.6 \text{ kJ}\cdot\text{mol}^{-1}$ , ref. 28) and hence, the result does not allow for a clear discrimination between a *metallic* and *noble-gas-like* behavior. The longer-lived isotope  $^{289}\text{Fl}$  could not be identified due to a high background from Rn isotopes and their decay products, disturbing an unambiguous identification of decay chains starting with  $^{289}\text{Fl}$ .<sup>27</sup> Both, nuclear as well as chemical aspects of the experiment reported in ref. 27 have been criticized, see ref. 29. The predicted similarity of a hypothetical *noble-gas-like* behavior of Fl to that of Rn calls for applying physical pre-separation methods to separate Cn and Fl from Rn. Its decay products caused the main background in the  $\alpha$  spectra in ref. 27. A first attempt using physical pre-separation was performed at the Dubna Gas-Filled Recoil Separator (DGFRS), but failed to observe Fl.<sup>30</sup> The question whether Fl resembles more closely a noble gas or a noble metal is

among the most pressing ones in concurrent superheavy element chemistry and needs to be solved experimentally in a more sensitive and detailed study.

Here, we report on chemical studies of Fl after preseparation with TASCA, which led to the observation of two Fl atoms.

## 2. Experimental

To isolate Fl we exploited a combination of the TransActinide Separator and Chemistry Apparatus<sup>25,31,32</sup> (TASCA) and the Cryo Online Multidetector for Physics And Chemistry of Transactinides (COMPACT).<sup>33</sup> TASCA served for suppression of the primary beam and of the background from Rn isotopes and their decay products. This allowed the observation of the characteristic radioactive decay of Fl and its (grand)-daughters under significantly improved background reduction compared to previous studies<sup>27</sup> performed without preseparation.

The gas chromatography and detection system comprised two COMPACT detector arrays which were placed behind TASCA. The experimental set-up is schematically shown in Figure 1.

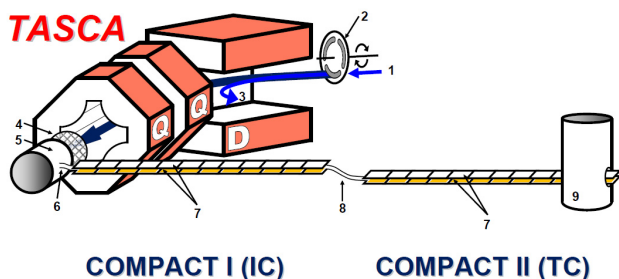


**Figure 1.** Schematic drawing of the TASCA-COMPACT<sup>2</sup> arrangement used for the gas chromatographic investigation of the volatility of Fl and its reactivity towards Au. The <sup>48</sup>Ca-beam (1) passed through the rotating <sup>244</sup>Pu-target (2) assembly. The separator TASCA consists of one dipole (D), where unwanted nuclear reaction products (3) were deflected, and two quadrupole (Q) magnets. At the exit of TASCA a vacuum window (4) separated the low-pressure required in TASCA from the high-pressure applied in the recoil transfer chamber (RTC) (5). After passing the vacuum window, Fl was thermalized in the gas inside the RTC and was transported in its elemental state with the carrier gas through a 2-cm long PTFE tube (6) into a series of two COMPACT detector arrays (7) connected by a 30-cm long polytetrafluoroethylene (PTFE) capillary (8) (2 mm i.d.). A negative temperature gradient was applied along COMPACT II using a liquid nitrogen cryostat (9) at the exit.

A <sup>48</sup>Ca<sup>10+</sup> beam of typically  $2 \cdot 10^{12}$  particles·s<sup>-1</sup> was accelerated by the UNiversal Linear ACcelerator (UNILAC) at the GSI, Darmstadt, Germany, to an energy of 259.4 MeV. In total, a projectile dose of  $4 \cdot 10^{18}$  particles was collected. The projectiles first passed through (2.50±0.05)-μm thick Ti target-backing foils, and then entered the <sup>244</sup>PuO<sub>2</sub> targets prepared by molecular plating and mounted on a rotating wheel.<sup>34,35</sup> The target wheel consisted of three segments (1.7 cm<sup>2</sup> area each) covered with 440 μg cm<sup>-2</sup>, 771 μg cm<sup>-2</sup>, and 530 μg cm<sup>-2</sup> <sup>244</sup>Pu, respectively. The isotopic composition was: 97.9% <sup>244</sup>Pu; 1.3% <sup>242</sup>Pu; 0.7% <sup>240</sup>Pu; <0.1% other. The target wheel rotated with 2000 rev min<sup>-1</sup> and was synchronized with the beam macrostructure to distribute each 5-ms long beam pulse evenly over one target segment.<sup>36</sup> In com-

plete nuclear fusion reactions <sup>292</sup>Fl\* compound nuclei at an excitation energy, E\*, of 40-45 MeV were formed.<sup>37,38</sup> After deexcitation by evaporation of three or four neutrons, the resulting <sup>288,289</sup>Fl nuclei recoiled from the target into the separator TASCA operated in the “Small Image Mode”.<sup>32</sup> The primary beam and unwanted nuclear reaction products were deflected inside the dipole magnet to a beam stop, while Fl was guided to the focal plane (Figure 1). Magnets were set to focus ions with a magnetic rigidity, B·ρ, of 2.27 T·m into a ~ (3 x 5) cm<sup>2</sup> area in TASCA's focal plane. Monte Carlo simulations indicate that 35% of the Fl ions reached this area.<sup>25,39</sup> There, they penetrated a (40x30) mm<sup>2</sup>-large MYLAR™ window of (3.3±0.1) μm thickness mounted on a 1-mm thick supporting grid of 80% geometrical transparency and entered the Recoil Transfer Chamber (RTC).<sup>31,40</sup> The window separated the low-pressure region in TASCA (0.5 mbar) from the high-pressure one in the RTC (~900 mbar). In the 29-cm<sup>3</sup> large RTC, made from polytetrafluoroethylene (PTFE), the Fl ions were thermalized in a dried (measured dew point below -60°C) gas mixture (He:Ar=70:30; gas purities: 99.9999% (He) and 99.999% (Ar)), which flushed the RTC at a total flow rate of 1300-1800 mL·min<sup>-1</sup>. The Ar admixture (30%) in the carrier gas served to increase the stopping power inside the RTC, which allowed minimizing the RTC volume. Short-lived Hg and Pb isotopes, chemical homologues of Cn and Fl, were produced using <sup>142</sup>Nd and <sup>144</sup>Sm targets, respectively. By producing pulses of <sup>182</sup>Hg recoils (0.4 s beam on and 50 s beam off) and measuring the time-delay until their decay in COMPACT, the most probable transport time to COMPACT I was determined to be (0.81±0.06) s at a gas flow rate of 1300 mL·min<sup>-1</sup>.

Volatile species including Fl, which was transported in its elemental state, were flushed with this carrier gas mixture through a 2-cm long PTFE tube (3 mm inner diameter, i.d.) into the first of the two COMPACT detector arrays (Figure 1). Each array consisted of 32 pairs (gap: 0.6 mm) of (1 x 1) cm<sup>2</sup>-large positive-intrinsic-negative (PIN) epitaxial silicon photodiodes with an active area of (9.7 x 9.8) mm<sup>2</sup> and an effective thickness of 150 μm. The calculated geometrical efficiencies for detecting an α particle or spontaneous fission from atoms present inside a detector array were 93% and ~100%, respectively. All detectors were covered by a (35-50)-nm thick gold layer deposited by evaporation. COMPACT I was operated as an isothermal chromatography (IC) detector array at room temperature (21 °C). It retained metallic elements that form a strong chemical bond with gold at room temperature, such as Pb or Hg. Chemical species that did not adsorb in COMPACT I exited, passed through a 30-cm long PTFE capillary (2 mm i.d.) and entered COMPACT II. COMPACT II was added five days after the start of the 29-day long experiment. A negative temperature gradient from +20 to -162 °C was applied along COMPACT II (thermochromatography detector array, TC) using a liquid nitrogen cryostat at the exit. For the first three days of operation, the lowest temperature in COMPACT II was -86 °C due to a weak thermal contact between the detector array and the cryostat. Volatile and inert elements pass COMPACT I and adsorb in COMPACT II at characteristic low temperatures. The energy resolution of the COMPACT detectors was ≅ 120 keV (FWHM). A higher resolution could not be reached because α particles are emitted isotropically at various angles in the narrow channel. Depending on their incident angle, they pass through different effective thicknesses of detector dead layer and gas, thus

undergoing energy loss to a different degree, before entering the active detector area. Accordingly,  $\alpha$  peaks show characteristic low-energy tailing. All transported species came in contact inside and downstream of the RTC exclusively with PTFE and gold surfaces. This set-up allowed for detecting species in a wide range of volatilities, namely from the low-volatile Pb to the noble gas Rn. If FI behaves like a metal it will adsorb in COMPACT I; if, in contrast, FI rather behaves like a noble gas, it will deposit at a much lower temperature in COMPACT II. The overall transfer yield from TASCAs to COMPACT was measured with short-lived Hg and Pb isotopes. To this end, the rate at which Hg atoms entered the RTC was determined by implanting them into a (58 x 58) mm<sup>2</sup> double-sided silicon strip detector. A subsequent experiment, in which the atoms were thermalized in the RTC and transported to COMPACT at a flow rate of 1300 mL·min<sup>-1</sup>, yielded that the decay of 27% of all Hg atoms entering the RTC was observed in COMPACT. For Pb isotopes this value was lower (20%), due to additional adsorption losses of the less volatile Pb on the walls of the RTC and the connecting tube. The distributions of <sup>182</sup>Hg and <sup>185</sup>Pb isotopes in COMPACT were measured before and after the FI measurement and found to be reproducible. Between these measurements, neither of the two COMPACT arrays mounted in the gas loop was opened. COMPACT II was warmed up every 2-3 days to remove the thin ice layer which formed on detectors held at temperatures below -75 °C.

### 3. Results

A search for correlated decay chains starting from <sup>288,289</sup>Fl was performed. The search conditions were the following: in case of <sup>288</sup>Fl, we searched for a 9.6-10.1 MeV  $\alpha$  particle, followed within 1 s by a >20 MeV fission fragment, which was registered in either the same or an adjacent detector pair, where the first  $\alpha$  particle was found. For <sup>289</sup>Fl, we searched for a 9.6-10.1 MeV  $\alpha$  particle, followed by a 8.8-9.3 MeV  $\alpha$  particle, followed by a >20 MeV fission fragment, all within 200 s. The search was extended to all detector pairs downstream of the one where the mother decay was observed, because the daughter of FI, Cn, is known to be a volatile metal and thus can be transported by gas flow along the detector channel. This procedure revealed two correlated decay chains, which we show in Figure 2.

Both members of chain #1 were observed in detector pair #9 in COMPACT I, which was kept at 21 °C. The members of chain #2 were found distributed over both COMPACT arrays: the  $\alpha$  particle of the mother nucleus initiating the chain was detected in detector #9 "top" in COMPACT I. The last two members of the chain were detected in detector pair #52 in COMPACT II at -32 °C. Based on the good agreement of the nuclear properties of our observed chains with decay properties reported from <sup>288,289</sup>Fl synthesis experiments<sup>4,23,25</sup>, we assign chain #1 to the decay of <sup>288</sup>Fl → <sup>284</sup>Cn and chain #2 to <sup>289</sup>Fl → <sup>285</sup>Cn → <sup>281</sup>Ds, produced in the 4n and 3n evaporation channel, respectively. A search for SF decays ( $E > 20$  MeV) revealed two additional events. In total, only these four SF events were registered - all with two coincident fission fragments. No "single" fission fragment with  $E_{\text{frag}} > 20$  MeV was detected. The SF events, for which no  $\alpha$ -decay precursor was found, appeared at temperatures of +21 °C (COMPACT I, det. 1T/1B, 83/83 MeV) and -86 °C

(COMPACT II, det. 64T/64B, 24/85 MeV). A definite assignment of these two SF events to a certain element is not possible as SF is an unspecific decay mode.

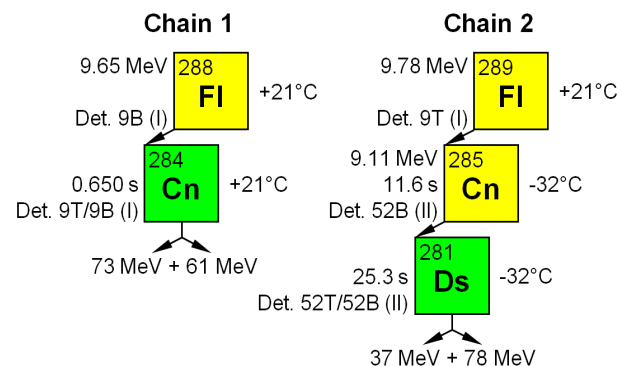


**Figure 2.** Observed correlated decay chains assigned to FI. Left-hand side of the boxes:  $\alpha$ -particle energy, lifetime of the nucleus, and detector number in which the signal was measured ("T" and "B" are top and bottom detectors of a detector pair, respectively). (I)/(II) denote COMPACT I and COMPACT II, respectively. Energies of SF fragments are given below the boxes. No pulse-height defect correction was applied to the SF energies. Right hand side of the boxes: temperature of the detector that registered the event.

The observed  $\alpha$  energies in the decay chains are somewhat lower compared to the energies registered in earlier experiments in a focal plane detector, into which the <sup>288,289</sup>Fl was implanted.<sup>22,23,25</sup> This is due to energy loss in the gas layer, which the  $\alpha$  particles penetrate in roughly half of all cases, and is in agreement with a long tail of  $\alpha$  peaks towards the low energy side (Figure 3). Such an effect was observed in all our previous chemistry experiments, where similar cryodetectors were used.<sup>17,33</sup> The asymmetric broadening of  $\alpha$  peaks towards low energy can be understood as being due to the energy loss of particles penetrating the gas channel at shallow angles.

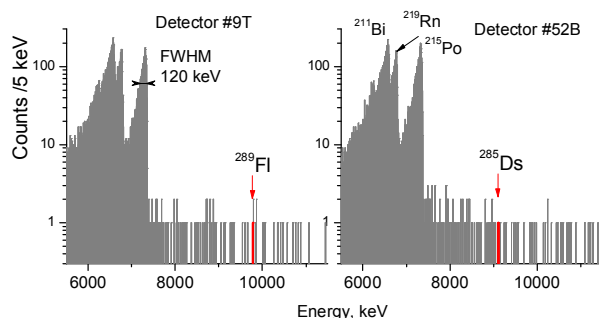


**Figure 3.** Spectra measured in detector #9T of COMPACT I (left panel) and detector #52B of COMPACT II (right panel) during 22 days.  $\alpha$  decays from <sup>289</sup>Fl and <sup>285</sup>Ds are shown in red.

Due to the extremely low background from  $\alpha$  particles and especially from SF fragments, the observed decay chains are highly significant. The probabilities for a random origin, unrelated to the decay of FI, are only  $6.3 \cdot 10^{-6}$  (chain #1) and  $1.3 \cdot 10^{-6}$  (chain #2). Figure 3 shows the total  $\alpha$  spectra measured during 22 days in detector #9T (COMPACT I) (left panel) and in detector 52B (COMPACT II) (right panel), where members of the second decay chain were registered.

The entries of two  $\alpha$  particles belonging to  $^{289}\text{Fl}$  and  $^{285}\text{Cn}$ , the members of chain #2, are marked, distributed over two COMPACT detectors. The only peaks visible in these spectra arise from the decay chain  $^{219}\text{Rn} \rightarrow ^{215}\text{Po} \rightarrow ^{211}\text{Bi}$ . Small amounts of  $^{219}\text{Rn}$  were added to the carrier gas to allow for an on-line monitoring of the detection system and to provide  $\alpha$  calibration data. No peaks are present in the spectra above the highest energy originating from the  $^{219}\text{Rn}$  chain, i.e., above 7.5 MeV. This illustrates nicely the power of physical pre-separation by a recoil separator in a chemistry experiment.

#### 4. Discussion

In Figure 4 we show the temperature profile in the main part of the experiment (panel a) together with the measured distribution (solid bars) of Pb (panel b), Hg (c) and Rn (d). Also shown are the positions at which the members of the two Fl decay chains were observed (e). Monte Carlo simulations<sup>41</sup> (MCS) of the migration of Pb, Hg, Rn, Cn and Fl along the chromatography detectors were performed with 10000 atoms for each element. The distribution pattern of Rn in COMPACT II was simulated using the literature value ( $-\Delta H_{ads}^{ice}(\text{Rn}) = 20 \text{ kJ}\cdot\text{mol}^{-1}$ , ref. 28). Pb and Hg interact strongly with Au ( $-\Delta H_{ads}^{Au}(\text{Pb}) > 295 \text{ kJ}\cdot\text{mol}^{-1}$  (ref. 42), and  $-\Delta H_{ads}^{Au}(\text{Hg}) = (98 \pm 3) \text{ kJ}\cdot\text{mol}^{-1}$ , (ref. 20)), and their deposition temperatures on a gold surface are well above room temperature. The similarity in the observed distribution patterns for Hg and Pb, which have significantly different adsorption enthalpies on gold, points at the diffusion-controlled nature of the adsorption process. The diffusion to the wall controls the process for both Pb and Hg, and they adsorb upon first contact with the surface at the beginning of COMPACT I. Using MCS a lower limit of  $-\Delta H_{ads}^{Au} > 64 \text{ kJ}\cdot\text{mol}^{-1}$  was deduced for both Pb and Hg.

In the following part we discuss the adsorption scenarios for the two Fl atoms. Both  $\alpha$  decays from Fl have been found in the IC section, where short-lived isotopes of the metallic elements Pb and Hg were deposited. For the unknown adsorption behavior of Fl, three possible cases can be discussed. (i) Fl is not very volatile and reacts strongly with Au. Then, the distribution pattern in COMPACT should be similar to that of its nearest lighter homolog Pb. However, both decays of Fl were found in the detector pair #9, while more than 90% of Pb was deposited on the first eight detector pairs. This fact points to a weaker reactivity of Fl with gold compared to Pb. (ii) Fl does not exhibit a metallic character but interacts with Au by weak dispersion forces. In that case, most of the Fl should pass COMPACT I and decay at low temperatures in COMPACT II. Decays inside COMPACT I, occurring predominantly due to decay-in-flight, will be distributed evenly along the whole detector array. Rn is a typical representative for such a behavior. It is not deposited until very low temperatures are reached. In fact, most of the Rn was flushed out after passing both COMPACT arrays. In this case, Fl decays would be predominantly detected in COMPACT II. (iii) Fl may behave as a volatile metal and decay upon the adsorption on Au in one of the two COMPACT arrays, with the deposition temperature and hence position depending on its adsorption enthalpy value, similar to a behavior observed for Cn.

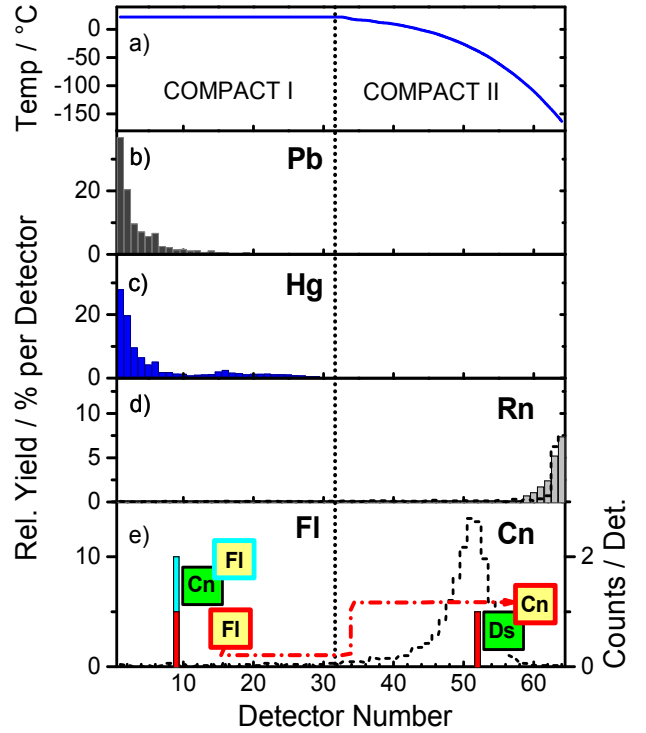


**Figure 4.** The observed gas-chromatography behavior of Fl and Cn in COMPACT compared to that of Pb, Hg and Rn. Measured distributions (bars) of  $^{185}\text{Pb}$  (panel b),  $^{182}\text{Hg}$  (panel c), and  $^{219}\text{Rn}$  (panel d) together with the temperature profile in the main part of the experiment (panel a) are shown. The positions where the  $\alpha$  particles from the members of the decay chains were observed are shown in (e): chain #1 – event in light blue in the histogram, corresponding to the light-blue bordered inserted box; chain #2 – events in red / red-bordered boxes. The fissions terminating the chains were observed in the same detector pairs as precursor  $\alpha$  particles from Fl in chain #1 or from Cn in chain #2. The dashed lines show the results of Monte Carlo simulations for Rn and Cn using literature values (ref. 28/ ref. 19) for  $-\Delta H_{ads}$ .

In chain #1 originating from  $^{288}\text{Fl}$ , the SF decay from  $^{284}\text{Cn}$  was registered, after a lifetime of 650 ms, in the same detector pair as the  $\alpha$  decay of the mother nuclide  $^{288}\text{Fl}$ . A  $^{284}\text{Cn}$  atom interacting with a gold surface with  $-\Delta H_{ads}^{Au}(\text{Cn}) = 52 \text{ kJ}\cdot\text{mol}^{-1}$  needs about 135 ms to be transported 1 cm downstream in COMPACT I by the carrier gas. Within 650 ms, a  $^{284}\text{Cn}$  atom, either residing adsorbed on the surface or being immersed in the gas would be transported a few centimeters downstream the detector channel. The fact that  $^{284}\text{Cn}$  remained at the same position during its entire lifetime is indicative for its implantation into the detector as a recoiling atom in the  $\alpha$  decay of  $^{288}\text{Fl}$ . This is expected in about 50% of all  $\alpha$  decays. It is due to the nuclear recoil from the nuclear decay of the mother atom with the  $\alpha$  particle being emitted away from the surface of the detector on which the mother atom is adsorbed. As the recoil range of  $\alpha$ -decay products is very small, this implies that indeed the mother atom,  $^{288}\text{Fl}$ , was adsorbed on the detector surface when it decayed, and that the position where the decay was observed is indicative of a chemical interaction of Fl with Au. In chain #2 originating from  $^{289}\text{Fl}$ , the last two members, starting from the daughter nucleus  $^{285}\text{Cn}$ , were found in detector pair #52 at a temperature of  $\sim 32 \text{ }^\circ\text{C}$ . Apparently, upon  $\alpha$  decay of the

mother nucleus, the daughter  $^{285}\text{Cn}$  recoiled into the gas stream. During its lifetime of 11.6 s, it was transported along the detector channel into COMPACT II. As shown in Figure 4(e), the observed adsorption position for  $^{285}\text{Cn}$  agrees well with the calculated deposition pattern for this Cn isotope using the experimentally measured adsorption enthalpy.<sup>19</sup> This corroborates our assignment of the last two members to  $^{285}\text{Cn} \rightarrow ^{281}\text{Ds}$  and hence that of the mother being  $^{289}\text{Fl}$ .

Both observed Fl decays were registered in the isothermal section, in COMPACT I, while zero decays were observed in COMPACT II. Considering the low experimental statistics, a method of calculating confidence intervals for experiments with small event numbers was applied.<sup>43</sup> The numbers of events, which were detected in COMPACT I and COMPACT II, are  $D=2$  and  $N=0$ , where we use the notation as in ref. 43. For the evaluation of confidence levels using Poisson statistics,  $D$  and  $N$  can vary from 0 to 2, with  $D+N=2$ . Lower ( $R_{lo}$ ) and upper ( $R_{hi}$ ) limits for the ratio  $R = N/D$  can be calculated for different confidence intervals, as well as the most probable value of  $R$ ,  $R_{max}$  (ref. 43). Thus, the upper limit  $R_{hi}$  corresponds to the maximum value of  $N$ ,  $N_{hi}$ , within the selected confidence interval, and therefore, to the minimum value of  $D$ ,  $D_{lo}$ . Similarly, the lower limit  $R_{lo}$  corresponds to the minimum value of  $N$ ,  $N_{lo}$ , and to the maximum value of  $D$ ,  $D_{hi}$ , within the selected confidence interval. From the experiment we obtained the most probable value of  $R$  as  $R_{max} = 0$ , resulting in limits  $R_{lo}=0$  and  $R_{hi}=1.650$  for the 95% confidence level (95% c.l.). These values correspond to  $N_{hi}=1.24$  and  $D_{lo}=0.76$ . Thus, the experimental values  $D$  and  $N$  are Poisson-distributed within the intervals:  $0.76 < D < 2$  and  $0 < N < 1.24$  at the 95% confidence level. The minimum value for the number of events  $D$ , which are detected in COMPACT I at this limit, is 0.76 out of 2, i.e., 38%. To

convert this into a limit for  $-\Delta H_{ads}^{Au}(Fl)$ , the deposition pattern for both observed Fl isotopes along the entire COMPACT array was simulated for various values of  $-\Delta H_{ads}^{Au}(Fl)$  using MCS<sup>41</sup>. All simulations with  $-\Delta H_{ads}^{Au}(Fl) \geq 48 \text{ kJ}\cdot\text{mol}^{-1}$  resulted in distributions where at least 38% of all events decayed in COMPACT I. Therefore,  $-\Delta H_{ads}^{Au}(Fl) > 48 \text{ kJ}\cdot\text{mol}^{-1}$  was found as a lower limit for the adsorption enthalpy of Fl on gold at 95% c.l. Similar calculations were performed for 90% and 68% confidence intervals, resulting in limits of 49 kJ/mol and 50 kJ/mol, respectively.

## 5. Conclusion

A gas phase chromatography experiment with Fl was performed. Two atoms were registered. The observed behavior of Fl in the chromatography column indicates that Fl is less reactive than Pb. The estimated minimum value of  $-\Delta H_{ads}^{Au}(Fl) > 48 \text{ kJ}\cdot\text{mol}^{-1}$  reveals a *metallic* character upon adsorption on Au due to the formation of a metal-metal bond, which is at least as strong as that of Cn.<sup>18,19</sup> The observed behavior is in agreement with results of recent fully-relativistic calculations on the adsorption of Fl on a Au surface<sup>13-15</sup>, but disagrees with an observation of adsorption of Fl on Au merely due to physisorption.<sup>27</sup> To conclude, the present experimental study has established that Fl is a *volatile metal*, the least reactive one in group 14. It is, however, not as inert as a noble gas, as was initially assumed from atomic calculations.<sup>7</sup>

## REFERENCES

- (1) Fricke, B. *Struct. Bond* **1975**, *21*, 89.
- (2) Pyykkö, P and Desclaux, J.P. *Acc. Chem. Res.* **1979**, *12*, 276.
- (3) Schwerdtfeger, P. & Seth, M. In: *Encyclopedia on Computational Chemistry*, Wiley, New York, Vol. 4, 1998.
- (4) Oganessian, Yu. *Radiochim. Acta* **2011**, *99*, 429–439.
- (5) Loss R. D. and Corish J. *Pure Appl. Chem.* **2012**, *84*, 1669–1672.
- (6) Türler, A. and Pershina, V. *Chem. Rev.* **2013**, *113*, 1237.
- (7) Pitzer, K.S. *J. Chem. Phys.* **1975**, *63*, 1032.
- (8) Eichler, B. *Kernenergie* **1976**, *19*, 307.
- (9) Oganessian, Yu. *et al. Phys. Rev. C* **2000**, *62*, 041604(R).
- (10) Eichler, B. *PSI Report 00-09*; Paul Scherrer Institute, Villigen, Switzerland 2000.
- (11) Miedema, A. R.; Nieuwenhuys, B. E. *Surf. Sci.* **1981**, *104*, 491.
- (12) Eichler, R. and Schädel, M. *J. Phys. Chem. B* **2002**, *106*, 5413–5420.
- (13) Pershina, V. *Radiochim. Acta* **2011**, *99*, 459.
- (14) Pershina, V.; Anton, J.; Jacob, T. *J. Chem. Phys.* **2009**, *131*, 084713.
- (15) a) Zaitsevskii, A.; van Wüllen, C.; and Titov, A. *Russ. Chem. Rev.* **2009**, *78*, 1173. b) Zaitsevskii, A. *et al. Phys. Chem. Chem. Phys.* **2010**, *12*, 4152–4156.
- (16) Hermann, A. *et al. Phys. Rev. B* **2010**, *82*, 155116.
- (17) Düllmann, Ch.E. *et al. Nature* **2002**, *418*, 859–862.
- (18) Eichler, R. *et al. Nature* **2007**, *447*, 72–75.
- (19) Eichler, R. *et al. Angew. Chem. Intl. Ed.* **2008**, *47*, 3262–3266.
- (20) Soverna, S. *et al. Radiochim. Acta* **2005**, *93*, 1–8.
- (21) Yakushev, A. *et al. Radiochim. Acta* **2003**, *91*, 433–437.
- (22) Oganessian, Y. *J. Phys. G* **2007**, *34*, R165–R242.
- (23) Düllmann, Ch.E. *et al. Phys. Rev. Lett.* **2010**, *104*, 252701.
- (24) Stavsetra, L. *et al. Phys. Rev. Lett.* **2009**, *103*, 132502.
- (25) Gates, J. M. *et al. Phys. Rev. C* **2011**, *83*, 054618.
- (26) Ellison P.A. *et al. Phys. Rev. Lett.* **2010**, *105*, 182701.
- (27) Eichler, R. *et al. Radiochim. Acta* **2010**, *98*, 133–139.
- (28) Eichler, B.; Zimmermann, H. P.; Gäggeler, H. W. *J. Phys. Chem. A* **2000**, *104*, 3126–3131.
- (29) Düllmann, Ch.E. *Radiochim. Acta* **2012**, *100*, 67–74.
- (30) Wittwer, D. *et al. Nucl. Instrum. and Methods B* **2010**, *268*, 28–35.
- (31) Düllmann, Ch.E. *Eur. Phys. J. D* **2007**, *45*, 75–80.
- (32) Semchenkov, A. *et al. Nucl. Instrum. Methods B* **2008**, *266*, 4153–4161.
- (33) Dvorak, J. *et al. Phys. Rev. Lett.* **2006**, *97*, 242501.
- (34) Eberhardt, K. *et al. Nucl. Instrum. and Methods. A* **2008**, *590*, 134–140.
- (35) Runke, J. *et al. J. of Radioanal. Nucl. Chem.* **2013**, in press, DOI 10.1007/s10967-013-2616-6.
- (36) Jäger, E. *et al. J. of Radioanal. Nucl. Chem.* **2013**, in press, DOI 10.1007/s10967-013-2645-1.
- (37) Ziegler, J. F. *Nucl. Instrum. Methods B* **2004**, *219*–220, 1027.
- (38) Myers, W. D.; Świątecki, W. *J. Nucl. Phys. A* **1996**, *601*, 141.
- (39) Gregorich, K.E. *Nuclear Instrum. and Methods A* **2013**, *711*, 47–59.
- (40) Even, J. *et al. Nuclear Instrum. and Methods A* **2013**, *638*, 157–164.
- (41) Zvara, I. *Radiochim. Acta* **1985**, *38*, 95–101.
- (42) Serov, A. *et al. Proceedings of the Seventh International Conference on Nuclear and Radiochemistry*, Budapest, Hungary, 24–29 August, 2008, ISBN 978-963-9319-81-3.
- (43) Brüchle, W. *Radiochim. Acta* **2003**, *91*, 71–80.

## AUTHOR INFORMATION

### Corresponding Author

\* Christoph E. Düllmann  
Johannes Gutenberg University Mainz  
Institute for Nuclear Chemistry  
Fritz-Strassmann-Weg 2  
55128 Mainz, Germany  
Tel: +49-6131-39-25852  
Fax: +49-6131-39-20811  
Email: duellmann@uni-mainz.de

### Present Addresses

<sup>∠</sup>Abteilung SHE Chemie, GSI Helmholtzzentrum für Schwerionenforschung, D-64291 Darmstadt, Germany

<sup>∗</sup>Nuclear Science Division, Lawrence Berkeley National Laboratory, Berkeley, CA 94720-8169, U.S.A

<sup>∗∗</sup>Department of Chemistry & Biochemistry, University of Berne, CH-3012 Berne, Switzerland; and Laboratory for Radiochemistry and Environmental Chemistry, Paul Scherrer Institute, CH-5232 Villigen, Switzerland

<sup>∗∗∗</sup>Advanced Science Research Center, Japan Atomic Energy Agency, Tokai, 319-1195 Ibaraki, Japan

Jan Dvorak: Sektion SHE Chemie, Helmholtz Institute Mainz, D-55099 Mainz, Germany

<sup>°</sup>Flerov Laboratory of Nuclear Reactions, Joint Institute for Nuclear Research, 141980 Dubna, Russian Federation

<sup>®</sup>Kerntechnische Anlagen, TÜV SÜD AG, 80686 München, Germany

### Author Contributions

The manuscript was written through contributions of all authors. All authors have given approval to the final version of the manuscript.

### Funding Sources

This work was supported by the German BMBF under contracts 06MT247I, 06MT248 and 06MZ223I. The Research Center "Elementary Forces and Mathematical Foundations" is gratefully acknowledged.

## ACKNOWLEDGMENT

We thank the ion source and accelerator staff for providing stable and intense beams, the GSI experimental electronic department for providing data acquisition and analysis software, and V. Pershina for valuable discussions. This work was supported by the German BMBF under contracts 06MT247I, 06MT248 and 06MZ223I. The Research Center "Elementary Forces and Mathematical Foundations" is gratefully acknowledged.

## ABBREVIATIONS

COMPACT, Cryo-Online Multidetector for Physics And Chemistry of Transactinides; IC, Isothermal Chromatography; MCS, Monte Carlo Simulation; PTFE, polytetrafluoroethylene; TASCA TransActinide Separator and Chemistry Apparatus; TC, Thermochromatography

## SYNOPSIS TOC

The electronic structure of superheavy elements ( $Z \geq 104$ ) and their chemical properties are dominated by relativistic effects. Recently two superheavy elements were recognized by the IUPAC and named *flerovium* (Fl,  $Z=114$ ) and *livermorium* (Lv,  $Z=116$ ). Fl is the heaviest element with which chemical experiments were performed, based on the observation of single atoms. Here, we report on experiments that help answering the long-standing question whether Fl behaves rather like a noble gas or like a metal.

The image shows a standard periodic table of elements. Element 114, Flerovium (Fl), is highlighted with a yellow box. The table includes element symbols, atomic numbers, and names. The periodic table is color-coded by groups: Group 1 (orange), Group 2 (yellow), Groups 13-18 (purple), Groups 3-10 (blue), Groups 11-12 (green), and Groups 13-18 (pink).

1 H	2 He																
3 Li	4 Be											5 B	6 C	7 N	8 O	9 F	10 Ne
11 Na	12 Mg	13 Al	14 Si	15 P	16 S	17 Cl	18 Ar										
19 K	20 Ca	21 Sc	22 Ti	23 V	24 Cr	25 Mn	26 Fe	27 Co	28 Ni	29 Cu	30 Zn	31 Ga	32 Ge	33 As	34 Se	35 Br	36 Kr
37 Rb	38 Sr	39 Y	40 Zr	41 Nb	42 Mo	43 Tc	44 Ru	45 Rh	46 Pd	47 Ag	48 Cd	49 In	50 Sn	51 Sb	52 Te	53 I	54 Xe
55 Cs	56 Ba	57-71 La Ce Pr Nd Pm Sm Eu Gd Tb Dy Ho Er Tm Yb Lu	72 Hf	73 Ta	74 W	75 Re	76 Os	77 Ir	78 Pt	79 Au	80 Hg	81 Tl	82 Pb	83 Bi	84 Po	85 At	86 Rn
87 Fr	88 Ra	89-103 Ac Th Pa U Np Pu Am Cm Bk Cf Es Fm Md No Lr	104 Rf	105 Db	106 Sg	107 Bh	108 Hs	109 Mt	110 Ds	111 Rg	112 Cn	113 Nh	114 Fl	115 Mc	116 Lv	117 Ts	118 Og